

# Inhomogeneities in Fluidization of Spherical Particle Beds with Non-Newtonian Polymer Solutions

I. MACHAČ, B. ŠIŠKA, and Z. LECJAKS

*Department of Chemical Engineering, Faculty of Chemical Technology,  
University of Pardubice, CZ-532 10 Pardubice*

Received 14 June 1999

The anomalous course of expansion of spherical particle beds fluidized with non-Newtonian polymer solutions has been investigated experimentally in dependence on rheological properties of the fluid. In the experiments, the expansion of beds of uniform glass and lead balls was measured in two perspex rectangular columns. The test liquids were solutions of glycerol (Newtonian fluids), and aqueous solutions of various polymers (non-Newtonian fluids). The typical courses of bed expansion of spheres of 2.7 mm and 5.0 mm in diameter in the column of width 0.8 cm were documented by video-recording.

It was confirmed that due to the shear-thinning and elasticity of the fluid, the uniform fluidization becomes an aggregative one and the bed expansion reduces. The relationship, which is based on Carreau viscosity model, was proposed for the estimation of the maximum bed voidage and the extent of bed expansion. An analysis of the bed voidage distribution for fluidization of glass spheres of 5 mm in diameter with glycerol and non-Newtonian solutions of Natrosol and Praestol was discussed as well.

The flow of liquids through fluidized beds of particles is encountered in a variety of industrial applications. In a number of cases, the liquid phase can exhibit complex rheological behaviour. Typical examples wherein the liquid displays non-Newtonian flow characteristics are biochemical reactors and reactors for catalytic polymerization.

In design calculations of liquid-solid fluidized bed reactors, the fluidized bed of particles is usually considered to be uniform. Our extensive measurements of expansion of beds of spherical particles fluidized with different kinds of non-Newtonian liquids showed that the expansion course depends in a great measure on rheological behaviour of the fluid [1–4]. For the fluidization with pseudoplastic and simultaneously elastic polymer solutions in creeping flow region, it has been observed that with the increasing fluid velocity, in dependence on the degree of fluid pseudoplasticity and elasticity, the uniform fluidization becomes to be unstable. Unlike Newtonian fluidization, the remarkable particle concentration inhomogeneities gradually create in the bed up to the state of bed channelling [3, 4]. At the same time, the measure of the bed expansion reduces due to that phenomenon. This unexpected reality, which is characteristic especially of fluidization with viscoelastic fluids in creeping flow region, is not generally accepted in the literature dealing with non-Newtonian fluidization up to now.

Our effort has been aimed at the investigation of the anomalous course of expansion of spherical par-

ticle beds fluidized with non-Newtonian polymer solutions in dependence on rheological properties of the fluid and on geometry of the test column [4–6]. Qualitative changes in the bed structure during fluidization are well observable visually in a test column of rectangular cross-section (“two-dimensional” bed). The results of our experimental investigation of the expansion course making use of video-recording the spherical particle bed expansion in these columns are presented herein.

## EXPERIMENTAL

In our experiments, the expansion of beds was measured in two perspex rectangular columns with dimensions 1.2 cm × 8 cm × 80 cm and 0.8 cm × 8 cm × 80 cm. The beds were composed of nearly uniform glass and lead balls, their diameter and density are given in Table 1. The height of the beds at the onset of fluidization was about 12 cm–16 cm. The distributor with free area of 15 % was used.

The test liquids were solutions of glycerol, and solutions of methylcellulose Tylose, hydroxyethylcellulose Natrosol, polyacrylamides Praestol, Separan, and Kerafloc (see Table 2). The flow curves of the liquids were measured on rotary cylindrical viscometer Rheotest 2 in the interval  $1.5 \text{ s}^{-1} \leq \dot{\gamma} \leq \text{s}^{-1}$ .

During bed expansion experiments, the dependence of fluidized bed height on liquid volume flow rate was measured. Making use of the bed height, the

**Table 1.** Characteristics of the Spherical Particles Used

Symbol	Material	Diameter/mm	Density/(kg m <sup>-3</sup> )
S 1	Glass	1.465 ± 0.025	2506
S 2	Glass	1.923 ± 0.045	2524
S 3	Glass	2.782 ± 0.035	2504
S 4	Glass	4.117 ± 0.050	2596
S 5	Glass	5.031 ± 0.071	2845
S 6	Lead	1.973 ± 0.083	11093

**Table 2.** Characteristics of Test Liquids, 20 °C

Liquid	Density	Power-law parameters			Carreau model parameters		
	$\rho$ /(kg m <sup>-3</sup> )	$n$	$K$ /(Pa s <sup><math>n</math></sup> )	Range $\dot{\gamma}$ /s <sup>-1</sup>	$\eta_0$ /(Pa s)	$\lambda$ /s	$m$
Glycerol							
93 %	1243	1	0.426		0.426	0	1
83 %	1231	1	0.191		0.191	0	1
54 %	1140	1	0.0076	—	0.0076	0	1
Tylose MH 4000							
1.2 %	1001	0.854	0.567	1.5—13.5	0.450	0.103	0.756
1.0 %	1001	0.738	0.332	8.1—27.0	0.180	0.048	0.729
Natrosol MR 250							
1.2 %	1003	0.757	0.842	1.5—16.2	0.590	0.126	0.608
Natrosol HHX 250							
0.45 %	1001	0.605	0.714	1.5—16.2	0.50	0.239	0.485
Praestol 2935							
0.5 %	1001	0.316	2.04	1.5—27.0	3.60	2.28	0.317
0.15 %	1000	0.437	0.603	1.5—48.6	0.30	0.413	0.390
Separan AP 40							
0.35 %	1000	0.391	1.30	1.5—72.9	2.50	2.65	0.377
Kerafloc A 4008							
0.15 %	999	0.359	0.844	1.5—72.9	1.50	2.07	0.357

bed voidage  $\varepsilon$  characterizing the expansion of the bed as a whole was determined. The terminal velocities of particles falling through test liquids were measured separately in a cylindrical perspex column of 4 cm in diameter. Reynolds number  $Re_{tc}$  reached in the experiments ranged from 0.01 to 30.

The typical courses of expansion of beds of particles S 3 and S 5 in the column of width 0.8 cm were documented by video-recording using movie camera Panasonic NV-MS4E.

The experimental procedure is described in more detail in the work [6].

## RESULTS AND DISCUSSION

### Rheological Characteristics of Test Liquids

From the relevant rheometric data (Table 2), parameters  $n$  and  $K$  of the power law

$$\eta(\dot{\gamma}) = K \cdot \dot{\gamma}^{n-1} \quad (1)$$

were determined. The values  $\eta_0$  of zero shear rate viscosity of polymer solutions were estimated by means of sphere terminal falling velocity measurements, which

were extrapolated to low shear rates. Next, the parameters  $\lambda$  and  $m$  of the Carreau flow model

$$\eta(\dot{\gamma}) = \eta_0 / [1 + (\lambda \cdot \dot{\gamma})^2]^{(1-m)/2} \quad (2)$$

were determined making use of the rheometric data measured in the whole interval of shear rates reached on the Rheotest. The examples of the power law and Carreau flow model parameters of the test liquids are given in Table 2.

Solutions of glycerol are Newtonian fluids, polymer solutions exhibit a different degree of shear-thinning and elasticity. The degree of shear-thinning of a liquid can be evaluated according to the value of its flow index  $n$ , the degree of elasticity can be roughly evaluated according to the value of time parameter  $\lambda$  of the Carreau flow model. The solutions of Tylose are slightly shear-thinning and nearly inelastic, the solutions of Natrosol exhibit a greater measure of shear-thinning and elasticity, the solutions of Separan, Kerafloc, and 0.5 % Praestol are highly shear-thinning and elastic.

### Expansion of Beds

The extent and course of expansion of beds flu-

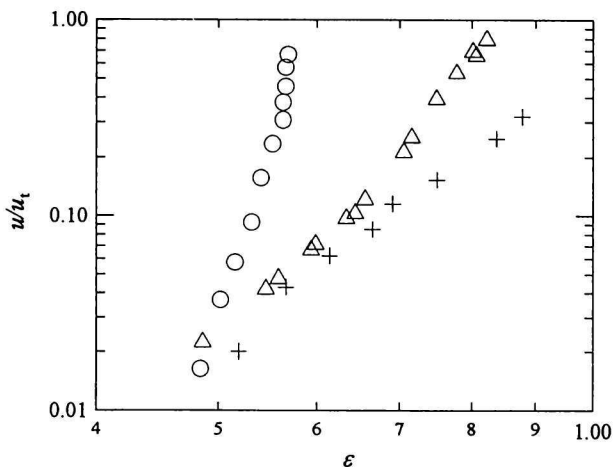


**Fig. 1.** Example of expansion curves for fluidization of particles S 3 with liquids of different measure of pseudoplasticity and elasticity in the creeping-flow region. + Glycerol 93 %,  $\Lambda_t = 0$ ;  $\Delta$  Natrosol MR 1.2 %,  $\Lambda_t = 1.6$ ;  $\circ$  Kerafloc 0.15 %,  $\Lambda_t = 20$ .

idized with liquids differing by their rheological behaviour have been evaluated according to the shape of expansion curves  $\log(u/u_t) = f(\log \epsilon)$ . Analyzing the results of experiments aimed at the investigations of wall effects on the fluidized bed expansion course in test columns with rectangular cross-sections, it was found out that the shape of expansion curves is similar to that obtained in cylindrical test columns. In both the cylindrical and rectangular test columns, the expansion curves of fluidization with viscoelastic fluids are due to increasing wall effects shifted to higher values of voidage but their shape is nearly unchanged [3, 4]. From here, it was deduced that the structures of beds fluidized in both test column geometries are similar as well and the rectangular cross-section boundaries have no significant influence on the quality of fluidization. Therefore, the columns of rectangular cross-section can be advantageously used for a fluidized bed structure observation [4].

At low Reynolds numbers, it was confirmed that with the increasing liquid volume flow rate and liquid pseudoplasticity and elasticity, the stability of the particulate fluidization decreases, fluidization becomes aggregative, the bed channelling manifests itself more and more evidently. Due to those effects, the bed expansion "rate" (the value of derivative  $d(\log \epsilon)/d(\log u)$ ) reduces.

In Figs. 1 and 2 the typical courses of expansion curves obtained for spherical particle beds fluidized with polymer solutions in columns of rectangular cross-section are shown for creeping- and transition-flow regions. In Fig. 3 the structures of beds of spherical particles S 3 fluidized with 93 % solution of glycerol, pseudoplastic and partly elastic 0.35 % solution of hydroxyethylcellulose Natrosol HHX, and with

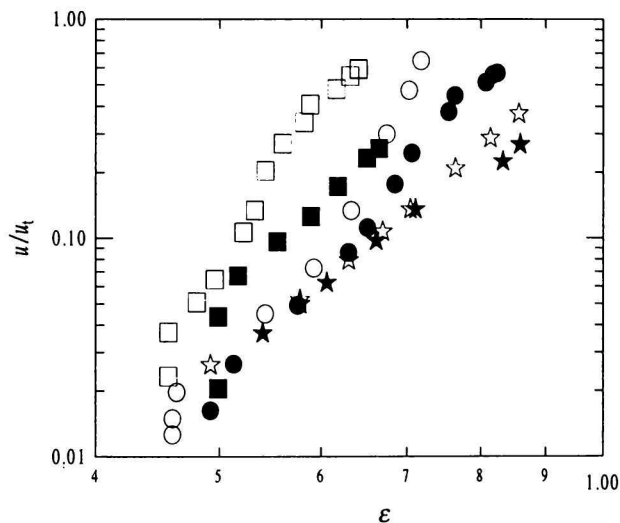


**Fig. 2.** Example of expansion curves for fluidization of spherical particles with liquids of different measure of pseudoplasticity and elasticity in the transition-flow region.  $\square$  Particle S 3 - Praestol 0.14 %,  $Re_{tc} = 2.2$ ;  $\blacksquare$  particle S 4 - Praestol 0.14 %,  $Re_{tc} = 9.5$ ;  $\circ$  particle S 3 - Natrosol HHX 0.45 %,  $Re_{tc} = 0.15$ ;  $\bullet$  particle S 4 - Natrosol HHX 0.45 %,  $Re_{tc} = 0.50$ ;  $\star$  particle S 3 - Tylose 1 %,  $Re_{tc} = 0.65$ ;  $\blackstar$  particle S 4 - Tylose 1 %,  $Re_{tc} = 1.9$ .

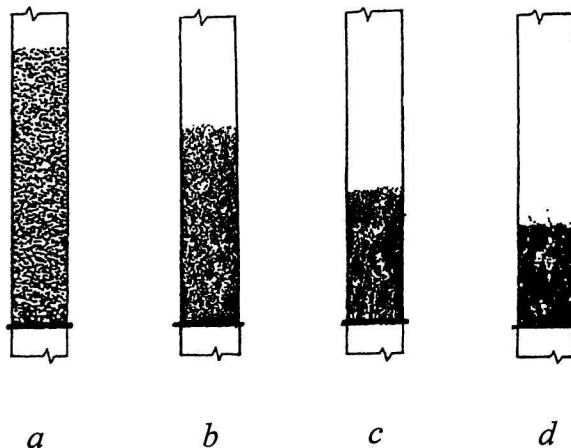


**Fig. 3.** Examples of structure of spherical particle beds for fluidization with different fluids. a Glycerol,  $u/u_t = 0.25$ ,  $\epsilon = 0.84$ ; b Natrosol HHX,  $u/u_t = 0.21$ ,  $\epsilon = 0.69$ ; c Praestol,  $u/u_t = 0.41$ ,  $\epsilon = 0.56$ ; d Kerafloc,  $u/u_t = 0.46$ ,  $\epsilon = 0.54$ .

strongly pseudoplastic and elastic 0.15 % solutions of polyacrylamides Praestol and Kerafloc are compared.

During observation of steady-state fluidization with glycerol, the bed of particles is roughly homogeneous in the whole interval of velocity ratio  $u/u_t$  measured. A similar picture of the bed expansion has been observed during fluidization with weakly pseudoplastic and nearly inelastic solutions of Tylose. During

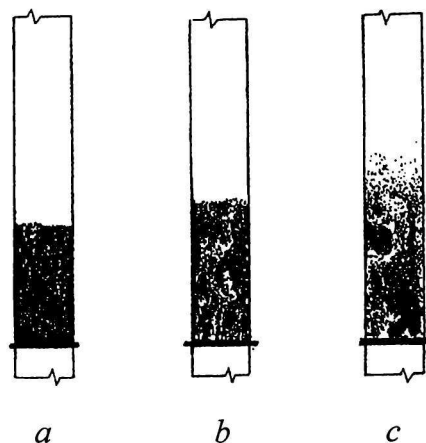


Fig. 4. Example of development of the bed structure in dependence on increasing fluid flow rate for fluidization with 0.15 % solution of Praestol. a  $u/u_t = 0.093$ ,  $\varepsilon = 0.51$ ; b  $u/u_t = 0.41$ ,  $\varepsilon = 0.56$ ; c  $u/u_t = 0.81$ ,  $\varepsilon = 0.59$ .

fluidization with more pseudoplastic and elastic solutions of Natrosol, random fluid voids and channels are created in the bed at higher values of fluid flow rate ( $u/u_t > 0.1$ ) and the extent of bed expansion decreases. In the beds fluidized with strongly elastic fluids (solutions of polyacrylamides), a set of relatively stable channels is created and the extent of the bed expansion achieved within the velocity ratio interval  $u_{mf}/u_t < u/u_t < 1$  is very small.

The development of the bed structure in dependence on the increasing fluid flow rate is shown in Fig. 4 for fluidization with 0.15 % solution of Praestol. At low values of the ratio  $u/u_t$  ( $u/u_t < 0.1$ ), the liquid flows through a greater number of relatively narrow channels, so that the bed structure does not differ markedly from that at the incipient fluidization. With the increasing fluid flow rate, due to the liquid bubbles formation, the number of channels decreases and their width enlarges. The individual particles inside the channel are drifted to the top of the bed and particle circulation becomes more intensive. At the high values of the ratio  $u/u_t$  ( $u/u_t \rightarrow 1$ ), the dimensions of the fluid voids and particle aggregates are growing and at the bed top a dilute region is forming from which individual particles are lifted to the top of column.

The results obtained are in qualitative accordance with aggregation and chaining of spheres observed during their sedimentation in viscoelastic fluids [7–9]. An unambiguous explanation of the mechanism of particle aggregation and channel creation does not exist, it is apparently a matter of combined effects of creation of liquid corridors with decreased viscosity due to the liquid pseudoplasticity, influence of normal stresses, and memory of the liquid.

Like the fluidization with polymer solutions in a cylindrical column [3], the bed expansion reduction

observed during fluidization in columns of rectangular cross-section weakens in transition-flow region and when a limiting value of Reynolds number, which depends on the degree of liquid elasticity, is exceeded, the elasticity effect vanishes and expansion curves become identical with those observed for Newtonian fluidization.

#### Extent of Expansion

Analyzing our experimental data, expansion equations based on power-law and Carreau flow models, which describe the anomalous bed expansion course, have been proposed for fluidization with pseudoplastic and elastic polymer solutions [1, 3–5]. The equations based on the Carreau flow model, which contains a time parameter  $\lambda$  connected with fluid elasticity, are more theoretically justified and yield better results in comparison with those based on the power law. However, the form of these equations and determination of Carreau model parameters are rather more complicated.

With respect to the course of experimental expansion curves in a log-log plot (Fig. 1), the expansion curves can be in the creeping flow region roughly approximated by two straight line segments within the velocity ratio subintervals  $u_{mf}/u_t < u/u_t \leq 0.12$  and  $0.12 < u/u_t < 1$ .

The segment courses can be described, for example, by the relationship

$$u/u_{oi} = (\varepsilon/\varepsilon_{oi})^{z_i} \quad (3)$$

where  $(\varepsilon_{oi}, u_{oi})$  are the coordinates of a characteristic point lying either on the bottom segment ( $i = 1$ ) or on the upper one ( $i = 2$ ) of the expansion curve,  $z_i$  are exponents corresponding to the slopes of the bottom or upper straight line segments in a log-log plot and depending on the rheological behaviour of fluid. The concrete forms of the relationship (3) describing the course of expansion curves in cylindrical and rectangular columns are given for fluidization with power-law and Carreau model fluids in works of Machač *et al.* [3–5].

In comparison with a particulate (homogeneous) fluidization, the bed channelling is connected with a reduction of the extent of bed expansion [10]. Therefore, the maximum value of bed expansion extent, determined as the ratio  $\varepsilon_{max}/\varepsilon_{mf}$  of the maximum bed voidage reached at  $u/u_t \rightarrow 1$  and the bed voidage at the onset of fluidization, can serve as a criterion of macrouniformity of the flow through fluidized bed.

Maximum value  $\varepsilon_{max}$  of the bed voidage depends on the fluid rheological behaviour and wall effects. In our non-Newtonian experiments in columns of rectangular cross-section, experimental values of the ratio  $\varepsilon_{max}/\varepsilon_{mf}$  were ranged in the interval from 1.06 for fluidization of particles S 2 with 0.15 % solution of

**Table 3.** Characteristics of Voidage Distributions in Beds Fluidized with Different Liquids

Liquid	$u/u_t$	$\varepsilon_m$	Direction	$\sigma/\varepsilon_m$
Glycerol	0.0948	0.73	horizontal	0.025
			vertical	0.040
			whole bed	0.082
	0.229	0.89	horizontal	0.026
			vertical	0.019
			whole bed	0.078
Natrosol HHX	0.0931	0.69	horizontal	0.034
			vertical	0.041
			whole bed	0.086
	0.351	0.86	horizontal	0.026
			vertical	0.040
			whole bed	0.073
Praestol	0.11	0.62	horizontal	0.033
			vertical	0.038
			whole bed	0.076
	0.83	0.74	horizontal	0.115
			vertical	0.099
			whole bed	0.166

Kerafloc (nearly totally channelling bed) to 2.17 for fluidization of particles S 3 with 1.2 % solution of Tylose (nearly particulate fluidization).

The value of maximum bed voidage can be in dependence on the Carreau model parameter  $m$ , dimensionless time parameter  $\Lambda_t$ , and ratio  $d/D_e$  of particle diameter and column effective diameter predicted from the relationship

$$\varepsilon_{\max} = \frac{1}{1 + 1.22\Lambda_t^{0.228}(1 - m) - 0.915m^{-1}(d/D_e)} \quad (4)$$

obtained by evaluating experimental data embracing the conditions  $0.36 \leq m \leq 0.87$ ,  $0.7 \leq \Lambda_t \leq 24$ ,  $0.45 \leq \varepsilon_{mf} \leq 0.48$ ,  $0.08 \leq d/D_e \leq 0.3$ , and  $Re_{tc} < 0.5$ .

#### Voidage distribution

For illustration, the video frames, which were recorded for expansion of beds of particles S 5 fluidized with 93 % glycerol, 0.45 % Natrosol HHX, and 0.5 % Praestol at conditions given in Table 3, have been analyzed on voidage distribution. To this purpose, the frame was divided into 64 units (matrix  $8 \times 8$ ) and the "local" voidage was determined by counting the number of particles present in each unit volume  $0.8 \text{ cm} \times 1.0 \text{ cm} \times 1.5 \text{ cm}$ . The experimental voidage interval was divided into 12 classes and the relative frequencies of each class were calculated making use of the local voidage data. Making use of the "local" voidage data obtained, the distribution measures, the

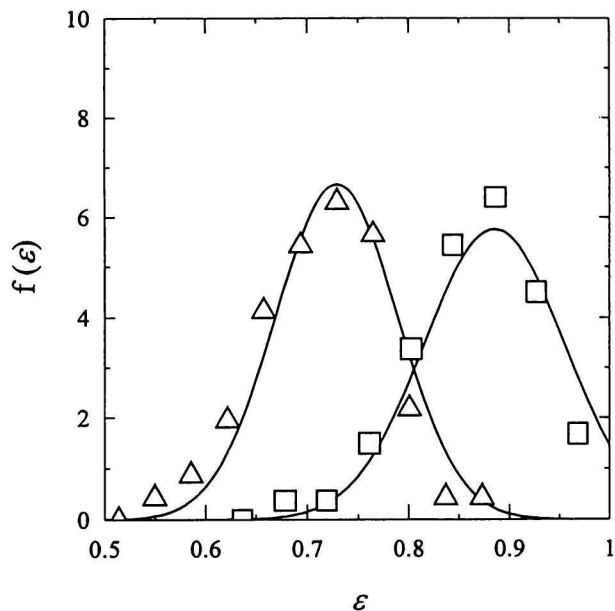


**Fig. 5.** Bed voidage distribution for fluidization of spherical particle S 5 with 93 % glycerol.  $\Delta$  Experimental data for  $\varepsilon_m = 0.73$ ;  $\square$  experimental data for  $\varepsilon_m = 0.89$ ; — normal probability distribution.

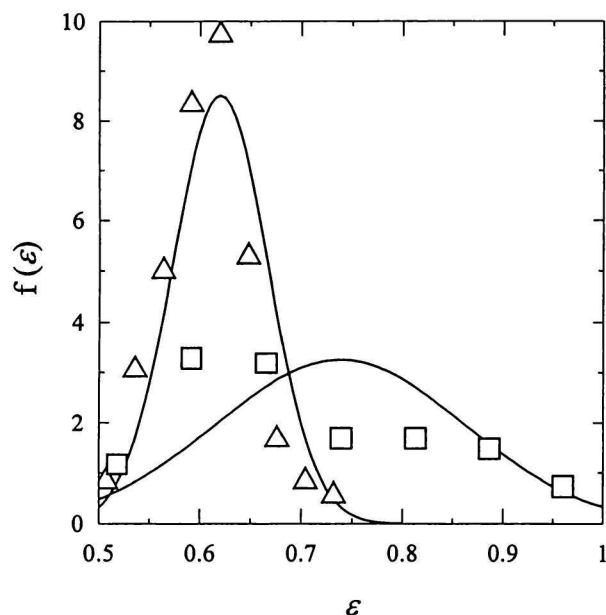


**Fig. 6.** Bed voidage distribution for fluidization of spherical particle S 5 with 0.5 % Praestol.  $\Delta$  Experimental data for  $\varepsilon_m = 0.62$ ;  $\square$  experimental data for  $\varepsilon_m = 0.74$ ; — normal probability distribution.

mean value  $\varepsilon_m$  and the standard deviation  $\sigma$ , were calculated for each voidage distribution as well. At the same time, the maximum deviation between the values of  $\varepsilon_m$  and the corresponding values of bed voidage calculated from the bed height, observed for fluidization with Praestol solution, was 2 %.

The resulting voidage distributions obtained for

fluidization with solutions of glycerol and Praestol are shown along with the theoretical normal probability distribution (full lines) in Figs. 5 and 6. Using the chi-square goodness-of-fit test on the significance level  $\alpha = 0.05$ , it was found that approximation of the experimental voidage distribution by the normal distribution can be accepted only for fluidization with Newtonian glycerol and medially shear-thinning solution of Natrosol at both investigated levels of expansion.

The bed structure inhomogeneity can be evaluated according to the value of the ratio  $\sigma/\varepsilon_m$  corresponding to a bed voidage distribution. In Table 3, besides the values of  $\sigma/\varepsilon_m$  characterizing the voidage distribution in the bed as a whole, the values characterizing the voidage distribution in vertical and horizontal directions of bed are also summarized. Inspecting the values of  $\sigma/\varepsilon_m$  given in Table 3, it can be concluded that, in contrast with our expectation, the measures of inhomogeneity of beds fluidized with Newtonian glycerol and medially shear-thinning solution of Natrosol are nearly the same and do not change with increasing flow rate. A remarkably greater degree of bed inhomogeneity is indicated only for the bed fluidized with strongly pseudoplastic and elastic solution of Praestol at the higher flow rate. At the same time, the degree of bed inhomogeneity in both vertical and horizontal directions does not differ significantly in all cases tested.

## CONCLUSION

The results of experimental investigations of anomalous expansion of spherical particle beds fluidized with shear-thinning and simultaneously elastic polymer solutions in rectangular test columns are presented. The changes in the bed structure connected with transition from particulate fluidization to aggregative one, due to fluid pseudoplasticity and elasticity, are documented by images obtained making use of corresponding video-records of fluidization.

The relationship based on the Carreau viscosity model has been proposed for the estimation of the maximum bed voidage and the extent of anomalous bed expansion.

Analyzing the bed voidage distribution for fluidization of glass spheres of 5 mm in diameter with glycerol and non-Newtonian solutions of Natrosol and Praestol, it was found that the approximation of the experimental bed voidage distribution by the normal distribution can be accepted only for fluidization with Newtonian glycerol and medially shear-thinning solution of Natrosol. The remarkable increase of the variance of the bed voidage distribution has been observed only for fluidization with strongly shear-thinning and elastic solution of Praestol at higher flow rate.

*Acknowledgements.* We would like to thank the Grant Agency of the Czech Republic for supporting our research work

performed in the frame of Grant Projects No. 104/95/1432 and 104/99/0992.

## SYMBOLS

$d$	particle diameter	m
$D_e$	effective column diameter	m
$K$	power-law parameter	Pa s <sup>n</sup>
$m$	Carreau flow model parameter	
$n$	power-law parameter (flow index)	
$Re_{tc}$	Carreau model Reynolds number $\left( = \frac{du_t \rho}{\eta_0} [1 + 0.25 \Lambda_t^2]^{(1-m)/2} \right)$	
$u$	superficial velocity	m s <sup>-1</sup>
$u_t$	particle terminal falling velocity in an unbound liquid	m s <sup>-1</sup>
$z$	exponent in eqn (3)	
$\dot{\gamma}$	shear rate	s <sup>-1</sup>
$\varepsilon$	bed voidage	
$\varepsilon_0$	characteristic bed voidage	
$\eta$	viscosity	Pa s
$\eta_0$	Carreau flow model parameter	Pa s
$\lambda$	Carreau flow model parameter	s
$\Lambda_t$	dimensionless time parameter $\left( = \frac{2\lambda u_t}{d} \right)$	
$\rho$	density	kg m <sup>-3</sup>

### Subscripts

$i$	related to a segment of expansion curve
$m$	mean value
$\max$	maximum value
$mf$	related to the onset of fluidization

## REFERENCES

1. Machač, I., Balcar, M., and Lecjaks, Z., *Chem. Eng. Sci.* 41, 591 (1986).
2. Machač, I., Mikulášek, P., and Lecjaks, Z., *Chem. Prum.* 37/62, 285 (1987).
3. Machač, I., Mikulášek, P., and Ulbrichová, I., *Chem. Eng. Sci.* 48, 2109 (1993).
4. Machač, I., Šiška, B., Lecjaks, Z., and Bena, J., *Chem. Eng. Sci.* 52, 3409 (1997).
5. Machač, I., Bena, J., and Šiška, B., *13th International Congress CHISA '98*, Prague, 1998.
6. Novotná, M., *Diploma Thesis*. University of Pardubice, 1998.
7. Allen, E. and Uhlherr, P. H. T., *J. Rheol.* 33 (4), 627 (1989).
8. Joseph, D. D., Liu, Y. J., Poletto, M., and Feng, J., *J. Non-Newtonian Fluid Mech.* 54, 45 (1994).
9. Šiška, B., Machač, I., Doleček, P., and Lecjaks, Z., *12th International Congress CHISA '96*, Prague, 1996.
10. Richardson, J. F., in *Fluidization*. (Davidson, J. F. and Harrison, D., Editors.) P. 25. Academic Press, New York, 1971.